Application of Optimal Experimental Design to Characterize Pressure Related Facility Effects in a Hall Thruster

Madison G. Allen*, Joshua Eckels†, Matthew P. Byrne ‡, Alex A. Gorodetsky§, and Benjamin A. Jorns¶
University of Michigan, Ann Arbor, MI, 48109

The method of Bayesian optimal experimental design (OED) is applied to calibrate a model for the response of plume distribution in a Hall effect thruster to facility pressure. An analytical model for the distribution of Hall thruster current density is developed that includes elements that represent a main beam, inelastically scattered ions, and charge exchange ions. The dependence of this model on facility pressure is formulated in terms of a series of free model parameters. Bayesian inference is employed to determine probability distributions for these model parameters from a set of 300 experimental data points previously generated [Diamant et, AIAA-2014-3710] for the SPT-100 Hall thruster. A method based on optimal experimental data with expected information gain is developed for calibrating the plume distribution model. As a proof of concept, this model is applied to the same SPT-100 data set, and it is shown that by employing this OED method, the same level of confidence in model parameters can be achieved with fewer experimental data points. This indicates a marked improvement in model training efficiency. This result is discussed in the context of limitations of the algorithm and future improvements.

I. Introduction

As the power of Hall effect thrusters continues to increase to meet the growing need for deep space mission applications, the problem of the test facility's influence on thruster operation becomes more acute. Indeed, one of the most well known effects is that background pressures in the facility can exceed on-orbit conditions by several orders of magnitude. [1] This problem becomes more pronounced as the power and flow rate of the engine increases, overwhelming the pumping capacity of the ground test facility.[2]

The presence of background pressure can impact the operation of the thruster in several ways. Notable examples include the shift in the location of the acceleration region and change in the divergence of the plume.[3] Background pressure also affects the cathode coupling voltage, as well as the strength of the discharge voltage oscillations.[4] In light of these effects, in order to qualify next generation propulsion systems for flight, there is a need to be able to find a way to correct for or alternatively map thruster operation from ground test to space-like conditions.

To this end, it has become a common practice to apply a parametric approach to extrapolate thruster performance to on-orbit pressures.[5] Researchers propose models of the facility effects then regress them on data sets of thruster operation as a function of pressure. These calibrated models are then extrapolated to the anticipated pressures in space. Historically, most models have been phenomenological, i.e. informed by the shape of trends in the data. Recent efforts have also started to investigate physics-based formulations for the thruster's response to facility effects.[6]

While this approach has been successfully applied for recent qualification efforts for thrusters up to 12.5 kW [7], there are possible issues leading to a decrease in confidence in this approach and the ability to accurately extrapolate to vacuum for higher power thruster operation (> 100 kW).[2] The higher output from high power thrusters leads to larger base pressures in the testing facility, so it is not possible to vary the background pressure in the same way and over the same order of magnitude as done with low power tests. This significantly diminishes the diversity of the data set. There also lies the challenge of probe accessibility in the testing facility that puts limitations on measurements and model accuracy. High power tests can damage the standard probes employed for plume characterization. In summary, the parametric approach can be curtailed at higher power as there are fewer operating conditions that can be accessed and

*Ph.D. Pre-Candidate, Department of Aerospace Engineering, mgallen@umich.edu
†Ph.D. Pre-Candidate, Department of Aerospace Engineering, eckelsjd@umich.edu
‡Ph.D. Candidate, Department of Aerospace Engineering, mpbyrne@umich.edu
§Assistant Professor, Department of Aerospace Engineering, goroda@umich.edu, AIAA Member
¶Associate Professor, Department of Aerospace Engineering, bjorns@umich.edu, AIAA Associate Fellow

less data can be generated. In light of these challenges, the need is apparent for optimizing the method of taking data to calibrate models with as little data as possible.

The goal of this paper is to investigate the method of optimal experimental design to calibrate models more efficiently for Hall thruster facility effects where as for a proof of concept, we consider a semi-empirical model for plume current density. To this end, this paper is organized in the following format. We first introduce our model of current density. We then review the method of OED and Bayesian inference and define the approach of the algorithm using the means of Expected Information Gain. In the next section, we describe a dataset drawn from previous work on the SPT-100 to test the algorithm and our model. In the following section, we apply the OED algorithm to this dataset and our model to evaluate its efficiency. In the final section, we discuss the implications of this approach in the context of improving testing speed and fidelity for extrapolating Hall thruster operation to orbit.

II. Theory

In this section, we give an overview of the model for plume divergence, and we introduce our algorithm for OED. This latter discussion requires a description of Bayesian inference and its relation to acquisition functions for optimizing pressure-related plume divergence experiments.

A. Reduced fidelity model for plume divergence

For this OED approach, we will first motivate a phenomenological based model for ion current density with respect to background pressure, P_B and position, (r, α). This approach is loosely based on the previous work of Randolph [8] and Goebel and Katz [1]. In this model, we assume the ion current density can be represented as the superposition of three components: the main beam of the plasma, j_b, ions created by inelastic scattering from neutrals, j_{scat}, and ions generated by charge exchange with neutrals j_{cex}. To this end, we propose the following model for the thruster plume distribution:

$$j(P_B, \alpha, r) = j_b(P_B, \alpha, r) + j_{scat}(P_B, \alpha, r) + j_{cex}(P_B, r), \tag{1}$$

where we have denoted the dependence of these properties on distance, r, from the thruster exit plane, background pressure in the facility, P_B, and angle, α, defined with respect to the centerline.

We adopt a semi-empirical approach to modeling each of these contributions. For both the beam and scattered populations, we assume the angular dependence can be described as normally distributed (Gaussian) with respect to angle and that the density decreases with solid angle, i.e. exhibiting a $1/r^2$ dependence. We thus have for the beam current density

$$j_b(P_B, \alpha, r) = \frac{I_B(r)}{r^2}\left(A_1 \exp\left[-\left(\frac{\alpha}{\alpha_1}\right)^2\right]\right) \tag{2}$$

$$j_{scat}(P_B, \alpha, r) = \frac{I_B(r)}{r^2}\left(A_2 \exp\left[-\left(\frac{\alpha}{\alpha_2}\right)^2\right]\right), \tag{3}$$

$$\tag{4}$$

where $I_B(r)$ denotes the total ion current carried by the beam and scattered populations, α_1, α_2 denote the characteristic divergence angles, and A_1, A_2 are normalizing constants. We define these as

$$A_1 = \frac{1 - c_0}{\frac{\pi^{3/2}}{2}\alpha_1\left(2\text{erfi}\left(\frac{\alpha_1}{2}\right) + \text{erfi}\left(\frac{i\pi - \alpha_1^2}{2\alpha_1}\right) - \text{erfi}\left(\frac{i\pi + \alpha_1^2}{2\alpha_1}\right)\right)} \tag{5}$$

$$A_2 = c_0\frac{1}{\frac{\pi^{3/2}}{2}\alpha_2\left(2\text{erfi}\left(\frac{\alpha_2}{2}\right) + \text{erfi}\left(\frac{i\pi - \alpha_2^2}{2\alpha_2}\right) - \text{erfi}\left(\frac{i\pi + \alpha_2^2}{2\alpha_2}\right)\right)}, \tag{6}$$

where we have introduced the additional constant, c_0. This constant, which is treated as a free parameter to be inferred from data, varies between 0 and 1 and ensures that the total current from the scattered and beam populations integrated over angle sums to I_B. It physically represents the ratio of current in the scattered beam to the main beam.

For our model for j_{CEX} , the charge exchange population, we assume this species expands spherically such that it is independent of angle:

$$j_{CEX}(P_B, r) = \frac{I_{cex}}{2\pi r^2}, \tag{7}$$

where I_{cex} is the total current carried by the charge exchange population. The form of this equation reflects the physical assumption that this slow moving population is effectively expanding in vacuum at the ion Bohm speed.

In Eqs. 2, 7, and 7, we relate the total currents by assuming that the two species are coupled through charge exchange collisions. This yields

$$I_B = I_{B(0)} \exp(-r n_n \sigma_{CEx}) \tag{8}$$

$$I_{cex} = I_{B(0)} \left(1 - \exp(-r n_n \sigma_{CEx})\right), \tag{9}$$

where σ_{CEx} is the cross-section of charge exchange collisions and the neutral density from the background facility pressure is represented by n_n. We assume this is approximately constant for the plume. This relationship physically captures the fact that charge exchange ions are born at the expense of the main beam/scattered populations.

Our overarching goal in formulating the preceding model is to try to represent how the current density distribution responds to facility pressure, i.e. the background neutral density. To this end, we introduce several ansatz about the scaling of key properties of the plume model with facility pressure. These include

$$\alpha_1 = c_1(c_2 \bar{P}_B + c_3) \tag{10}$$

$$\alpha_2 = c_2 \bar{P}_B + c_3 \tag{11}$$

$$n_n = c_4 \bar{P}_B + c_5. \tag{12}$$

where $\bar{P}_B$ denotes a facility pressure normalized by a constant value–typically the highest pressure measured during a parametric test. The constants c_1, c_2, c_3, c_4, c_5 represent model parameters that must be inferred from comparing the current density model to data.

Physically, the first two lines in Eq. 12 represent the fact that we assume the divergence angle is impacted by facility pressure. This has in fact been observed experimentally in previous studies [3], where typically the divergence decreases with higher facility pressure. While the physical mechanism driving this dependency is unknown, we chose to represent it phenomenologically in our formulation by assuming a simple linear scaling with pressure. Indeed, empirically, it has been shown in past work that for sufficiently low pressures, this relationship is in fact valid [4].

In addition to assuming the divergence scales with background pressure, we also make the strong assumption that the ratio of the divergences of the beam and scattered populations is constant, i.e. $\alpha_1/\alpha_2 = c_1/c_2$. This physically equates to the interpretation that the main current distribution that originates from the thruster is already comprised of both main beam and scattered ions. The divergence of both in turn are assumed to be impacted by pressure in the same way. The relative divergence of the scattered beam, however, by assumption is always larger than the main beam, i.e. $\alpha_2 > \alpha_1$. Finally, we note for the last line in Eq. 12 that we assume the average background neutral density in the plume also scales linearly with pressure.

In summary, for our semi-empirical model motivated in the preceding, there are six 6 unknown model parameters, $\{c_0, c_1, c_2, c_3, c_4, c_5\}$. In turn, there are three "design parameters" that can be manipulated to evaluate the model at different locations, $\{P_B, \alpha, r\}$. Our ultimate goal is to employ experimental measurements of current density at different sets of design parameters and to regress this data to find values of the model parameters. In turn, we can use this calibrated model to extrapolate to on-orbit conditions. With this in mind, we discuss in the following section our method to performing this model regression and how the approach of optimal experimental design can be employed to increase the efficiency of the regression.

B. Overview of Bayesian inference

The major challenge in applying the ion current density model is determining the model fitting parameters, denoted as $\theta = \{c_0, c_1, c_2, c_3, c_4, c_5\}$. To this end, it is necessary to regress data sets, $d = \{(x_1, y_1), (x_2, y_2), ...(x_n, y_n)\}$ where x_i denotes the independent variables of the model, y_i denotes the experimental observation, and n is the number of experiments performed. In our case, the independent variables are background pressure and position, $x_i = \{P_i, \alpha_i, r_i\}$. The experimental output of the model is local ion current density, $y_i = j_i$.

Our approach to regressing datasets to infer model parameters is based on Bayesian inference. In this case, we treat our knowledge of model parameters probabilistically and seek a posterior distribution, $P(\theta \mid d)$, that reflects our relative

confidence in the values of these model parameters given the measured data d. This posterior is obtained by updating our prior beliefs via data using Bayes' rule

$$P(\theta \mid d) = \frac{P(d \mid \theta)P(\theta)}{P(d)}, \tag{13}$$

where $P(\theta)$ is the prior, $P(d \mid \theta)$ is the likelihood, and $P(d)$ is the evidence. The prior distribution represents all prior knowledge about the model parameters prior to seeing the data. The likelihood captures the model relationship between the parameters and the data. Assuming independent experiments and Gaussian noise, the likelihood is

$$P(d \mid \theta) \propto \prod_{i=1}^{n} \exp\left(-\frac{(y_i - M(x_i, \theta))^2}{2\sigma_i^2}\right), \tag{14}$$

where $M(x, \theta)$ denotes the model,given by Eq. (1), and σ_i is the standard deviation of the measurement noise of the current density. Finally, the evidence provides a metric for how well the model fits the data on average, and can be explicitly written as the expected likelihood over the prior distribution.

As more data is obtained, the posterior distribution typically begins to converge to the best fit of the model parameters, i.e. a value with very little uncertainty. Unfortunately, to reach this level of confidence, it may be necessary to perform several experimental measurements. Indeed, the number of required experiments increases non-linearly with the number of model parameters. Direct experiment measurements of thruster plume properties, however, can become costly, especially for Hall thruster tests that may require altering backpressures in the vacuum chamber and moving probes throughout the entire expanse of the plume. Faced with this limitation, ideally, we need a methodology to determine the data points that have the highest potential value for increasing our confidence in the model parameters. This ultimately is the purpose of the OED algorithm, which we describe in more detail in the following section.

C. Optimal Experimental Design with Bayesian Inference

We take an information theoretic approach to optimal experimental design. Our goal is to determine the experiments that are *maximally informative* for the purposes of learning the parameters. In this respect, we seek designs that would maximize some difference between the prior and posterior distributions because the more informative the data is, the greater the difference between prior and posterior.

This approach to Bayesian optimal experimental design uses the KL divergence between prior and posterior to measure the amount of information gained by an experiment [9]. However, because an exact posterior is not available prior to actually running the experiment, the KL divergence is averaged so that we obtain an optimization objective called the *expected information gain*.

To motivate this approach, we recall the expressions for the differential entropy of distribution $H(P(\theta))$ and the cross entropy $H(P(\theta \mid y), P(\theta))$ between two distributions[10]:

$$H(P(\theta)) = \mathbb{E}_{P(\theta)}[-\ln P(\theta)] = -\int_{\Theta} P(\theta) \ln P(\theta) d\theta \tag{15}$$

$$H(P(\theta \mid y), P(\theta)) = \mathbb{E}_{P(\theta|y)}[-\ln P(\theta)] = -\int_{\Theta} P(\theta \mid y) \ln P(\theta) d\theta, \tag{16}$$

where $\mathbb{E}_{P(\theta)}[f(\theta)]$ denotes the expectation of f under distribution $P(\theta)$. We briefly recall that the entropy of a distribution measures the amount of uncertainty. For example, a normal random variable has entropy that scales linearly with the logarithm of the standard deviation. When data is obtained, entropy is removed from the system and thus information is gained.

Information gain, or KL divergence, from running an experiment at input x is obtained by subtracting the cross entropy from the entropy.

$$IG(x) = KL(\text{Posterior} \mid\mid \text{Prior}) = H(\text{Posterior}) - H(\text{Posterior}, \text{Prior}) = \int_{\Theta} P(\theta \mid x, y) \ln \frac{P(\theta \mid x, y)}{P(\theta)} d\theta. \tag{17}$$

The information gain is not computable since the data is not available. Thus the OED procedure seeks to perform an experiment that maximizes the *expected* information gain [9]

$$EIG(x) = \mathbb{E}_{P(y)}[IG] = \int_Y \int_{\Theta} P(y) P(\theta \mid x, y) \ln \frac{P(\theta \mid x, y)}{P(\theta)} d\theta dy = \int_Y \int_{\Theta} P(\theta) P(y \mid \theta, x) \left(\ln P(y \mid \theta, x) - \ln P(y \mid x)\right) d\theta dy \tag{18}$$

where the second equality results from a rearrangement using Bayes' rule.

As a result, the expected information gain requires the evaluation of a high-dimensional integral for which an analytic solution typically does not exist. The approach of [9, 11] relies on nested Monte Carlo sampling. To this end, recall that the marginal likelihood is an expectation over the prior $P(y) = \int_\Theta P(\theta)P(y \mid \theta)d\theta = \mathbb{E}_{P(\theta)}[P(y \mid \theta)]$, so that Monte Carlo estimator is obtained by sampling from the prior.

$$EIG(x) = \frac{1}{n}\sum_{i=1}^{n}\left(\ln P(y^{(i)} \mid \theta^{(i)}, x) - \ln \frac{1}{m}\sum_{j=1}^{m}\left(P(y^{(i)} \mid \theta^{(i,j)}, x)\right)\right). \tag{19}$$

While the samples $\theta^{(i)}$ and $\theta^{(i,j)}$ are obtained from the prior, the samples of the potential observations can be obtained by sampling from the Gaussian $\mathcal{N}(M(\theta, x), \sigma^2)$. This estimator is evaluated for each possible x in our design space to find the maximum of the estimated information gain which will be the location of the optimal data to measure. The nested sampling process for determining the Expected Information Gain for a single x is demonstrated below.

Algorithm 1: Expected Information Gain

for *i in n* **do**
- Sample $\theta^{(i)} \sim P(\theta)$;
- Evaluate $M(\theta^{(i)}, x)$;
- Sample $y^{(i)} \sim \mathcal{N}(M(\theta^{(i)}, x), \sigma^2)$;
- Evaluate likelihood $P(y^{(i)} \mid \theta^{(i)})$;
- **for** *j in m* **do**
  - Sample $\theta^{(i,j)} \sim P(\theta)$;
  - Evaluate the likelihood $P(y^{(i)} \mid \theta^{(i,j)})$;
- **end**

end

We employ a conclusion developed by [11] that reduces the cost of this generally expensive sampling procedure by utilizing the same samples of θ to calculate the likelihood and the estimator for the marginal likelihood. This has been proven to introduce minimal bias that does not significantly impact the optimization of function. In the next section we apply this approach to experimental data from a Hall thruster.

III. Results

In this section, we demonstrate the OED algorithm executed on ion current density data measured by Diamant et al. parametrically as a function of pressure in the L3 test facility [3]. Our overarching goal is to evaluate whether we can achieve the same level of confidence in model parameters, θ, with only a subset of the data that was originally collected by Diamant. This ultimately serves as a proof-of-concept of the OED algorithm.

To this end, we note that the SPT-100 data was measured using a probe arm swept at a fixed radial distance of 100 cm across the plume of the Hall thruster $[-90°, 90°]$. Since the ion current density model is a function of the radial distance but the SPT-100 data assumes a constant value, we similarly restrict our design space to only two inputs $x = P_B, \alpha$. The L3 data in turn consists of 8 pressure values each with at least 37 polar angle measurements for each pressure. We note here that we have normalized the pressure data from Ref. [3] to the maximum value from this dataset.

As a starting point, we first perform standard Bayesian inference using a Metropolis Hastings Markov Chain Monte Carlo (MHMCMC) scheme to sample the posterior distribution for all the SPT-100 data. This serves to provide a benchmark for comparison with the OED algorithm. To this end, we assume the prior distributions for all model parameters are uniform. We select the range for $c_0 \in (0, 1)$ to ensure that the beam is not artificially attenuated by CEX. We in turn select the range $c_1 \in (0.1, 0.5)$ to ensure effectively that the divergence of the main beam is always smaller than the scattered beam, i.e. $\alpha_1 < \alpha_2$. For the remaining parameters, we provide a large and relatively restricted range, e.g.$\{c_2, c_3, c_4, c_5\} \in (-200, 200)$.

After assuming these priors and applying our MCMC sampling algorithm, we show in Fig. 1c the results of the model prediction generated from the mean values of model parameters inferred from the posterior distribution. We also show for comparison as black points the locations of all the samples from the design space that were employed to inform

this model. As was discussed in the preceding, this model shows the broadening of the distribution with decreasing pressure, which in turn relates physically to an increase in divergence. Since the model is ultimately analytical, we in turn are able to project it to zero pressure.

We show as the right column in Fig. 2 the marginalized posterior distributions for the six free parameters. As can be seen, in all cases, the distributions are approximately normal and characterized by well-defined median values and variances. The relative departure of these distributions from the initial uniform priors suggests that the model is informative for determining these values.

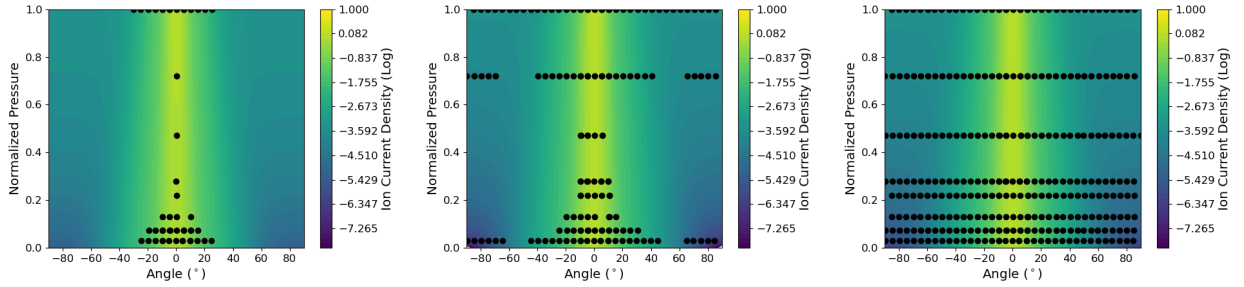

Fig. 1 Model predictions based on the mean values for the current density as a function of angle from thruster centerline and facility pressure for a) OED algorithm with N = 50 data points, b) OED algorithm with N = 150 data points, and c) the full dataset.

Now that we have established the baseline for comparison, we evaluate parametrically the performance of the OED algorithm. To this end, following our prescription from the previous section, we initialize the algorithm with the same priors we used to generate Figs. 1c. We next evaluate the EIG at each design point that exists in the SPT-100 dataset and select the one with the highest value. We then add this data point to the optimal dataset and update the posterior. With this posterior, we repeat the process using the posterior as a new prior for EIG evaluation and add an additional data point. Following this process, we show in Fig. 1a and b the model predictions with the expected values for $N = 50$ and $N = 150$. We also show on these plots as black points the locations of design parameters identified with the EIG algorithm.

It is evident from this plot that with only a subset of the data points, the OED algorithm is able to converge quantitatively to the same model shape and same model predictions to zero pressure. This is a strong initial proof of concept illustrating the utility of this technique. To this point, we also show as the first and second columns in Fig. 2 the marginalized posterior distributions with increasing number of points. This plot reveals that these distributions also rapidly converge to the results of the full dataset with only a subset of the data points.

To better quantify the trends in the model parameters, we show in Fig. 3 the variance in each model parameter as a function of number of iterations of the OED algorithm. These variances are estimated from the widths of the marginalized distributions (Fig. 2). As can be seen, as the number of iterations increases, the variance in all the model parameters decreases. In effect, this suggests that for this model, we may be able to achieve the same level of model parameter confidence with 50% of the dataset that was originally generated.

IV. Discussion

In this work, we have shown as a proof concept that an OED algorithm can in principle enable a more rapid convergence in model confidence and predictions for a semi-empirical model of the response of thruster current density to facility pressure. With that said, we remark that the actual application of the approach as we have performed here is impractical. We outlined the OED algorithm to select effectively any point in design space. In practice, this would require changing pressure and probe angle for every measurement. In some cases, the algorithm even suggests rapid changes between pressure values to reach specific positions and reverting the facility pressures back to previous values. This is impractical for real systems as pressure changes can require multiple hours to implement whereas angular probe changes are relatively quick and inexpensive. To introduce additional fidelity and utility into the algorithm, we will need to consider the relative costs of different measurements. This in effect can be accomplished by weighting the

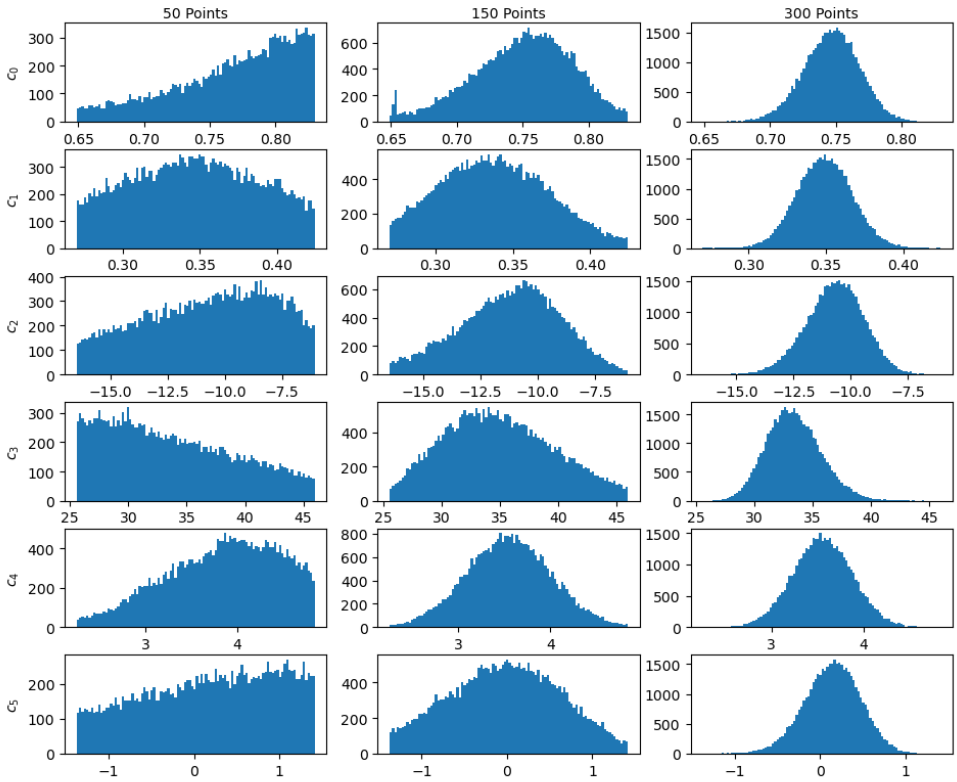

Fig. 2 Posterior distributions for the fit coefficients for $N = 50$ data points (left column), $N = 150$ data points (middle column), and the full dataset (right column) for c_0 (first row), c_1 (second row), c_2 (third row), c_3 (fourth row), c_4 (fifth row), and c_5 (sixth row)

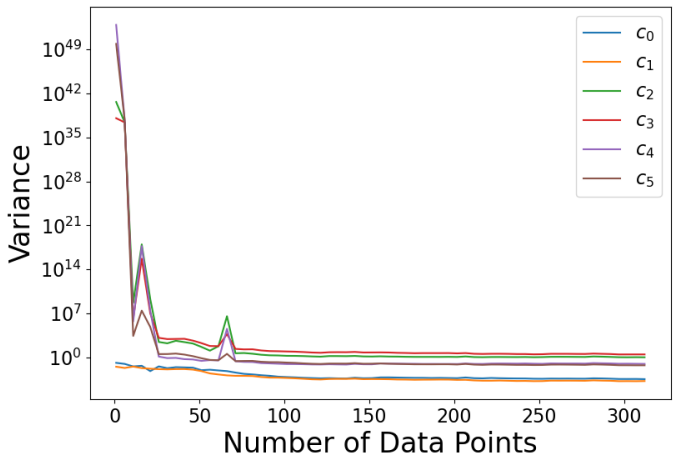

Fig. 3 Model parameter variance as a function of iterations of the OED algorithm.

acquisition function, e.g. by assigning more value to points that are closer in pressure. Moreover, as we investigate testing thrusters with exceeding high power levels, weights will need to be assigned based on the potential threats to probe lifetime by plume impingement. Ultimately, this type of weighting approach to the acquisition function is beyond the scope of this work but may be a promising next step for the advancement of this method. Indeed, ultimately, we envision integrating this method directly into the experimental campaign such that it can be employed in real time to dictate the next measurement location.

V. Conclusion

In this work, we have demonstrated that OED can be employed to more efficiently calibrate a model for the response of ion current density model to facility pressure. This model, which is largely phenomenological, accounts for beam ions, inelastically scattered ions, and charge exchange. We showed that by calibrating this model against an existing dataset [3] of current density as a function of pressure in the SPT-100, we were able to achieve the same level of confidence in the model predictions and parameters with only 50% of the full dataset. While we have remarked that this proof of concept as we have described it here is not practical–as it requires the ability to rapidly maneuver between pressures and probe locations—it is a positive initial proof that OED may be a valuable tool for future modeling and experimentally based efforts to extrapolate ground tests to flight. Indeed, this approach is particularly beneficial for the future of modeling facility effects for high-power Hall thrusters where there is limited design space of pressure values and positions.

References

[1] Goebel, D., and Katz, I., *Fundamentals of Electric Propulsion*, 2008.

[2] Hall, S., Cusson, S., and Gallimore, A., "30-kW Performance of a 100-kW Class Nested-channel Hall Thruster," *2015 International Electric Propulsion Conference*, 2015.

[3] Diamant, K., Liang, R., and Corey, R., "The Effect of Background Pressure on SPT-100 Hall Thruster Performance," *50th AIAA/ASME/SAE/ASEE Joint Propulsion Conference*, 2015.

[4] Huang, W., Kamhawi, H., and Lobbia, R., "Effect of background pressure on the plasma oscillation characteristics of the HiVHAc Hall thruster," *Physics of Plasmas*, 2019.

[5] Byrne, M., and Jorns, B., "Data-driven Models for the Effects of Background Pressure on the Operation of Hall Thrusters," *2019 International Electric Propulsion Conference*, 2019.

[6] Mikellides, I. G., Ortega, A. L., Chaplin, V. H., Snyder, J. S., and Lenguito, G., "Mechanism Behind the Dependence of Thrust on Facility Backpressure and Implications on the Operation of the SPT-140 Onboard the Psyche Mission," *2019 International Electric Propulsion Conference*, 2019.

[7] Huang, W., Kamhawi, H., and Haag, T., "Facility Effect Characterization Test of NASA's HERMeS Hall Thruster," *52nd AIAA/ SAE/ ASEE Joint Propulsion Conference*, 2016.

[8] Randolph, T., Kim, V., Kaufman, H., Kozubsky, K., Zhurin, V., and Day, M., "Facility effects on stationary plasma thruster testing," *23rd International Electric Propulsion Conference*, 1993.

[9] Ryan, K. J., "Estimating Expected Information Gains for Experimental Designs With Application to the Random Fatigue-Limit Model," *Journal of Computational and Graphical Statistics*, 2003.

[10] Gray, R. M., "Entropy and Information Theory," 2013.

[11] Huan, X., and Marzouk, Y. M., "Simulation-based optimal Bayesian experimental design for nonlinear systems," *Journal of Computational Physics*, 2013.